Event-triggered Feedforward Control subject to Actuator Saturation for Disturbance Compensation*

Takuya Iwaki[1], Junfeng Wu[2] and Karl Henrik Johansson[1]

Abstract— Feedfoward control is widely used to compensate measurable external disturbances. This paper studies feedforward control using an event-triggered sensor. Stability conditions when the feedback control is subject to actuator saturation are derived. We also obtain stability conditions of event-triggered feedforward control with anti-windup compensation. A numerical example shows that event-triggered feedforward control significantly reduces communication between the sensor and the controller without performance degradation compared with continuous-time feedforward control.

I. INTRODUCTION

Compensating external disturbances is one of the most important role of feedback control systems. The controller takes corrective action when the controlled variable deviates from its set-point, for instance, due to an external disturbance. However, disturbance compensation is unsuccessful when the time constant of the closed-loop system is too large. To improve the performance in this situation, feedforward control [1], [2] is widely used when the disturbance can be measured directly, for example, in process control [1], aircraft control [3], and active vehicle suspension [4]. By measuring disturbances, the control system can take corrective action before the disturbance affects the controlled variables. Thus, adding feedforward control is a promising way to improve control performance against external disturbances.

Event-triggered control has received much attention from both academic and industrial communities [5]–[7]. The main motivation for event-triggered feedback control is to reduce communication among the system components. Event-triggered PID control is discussed by many research groups [8]–[15]. As presented in [8], event-triggered PID control can significantly reduce the communication effort with only slight or no degradation of control performance.

Some practical problems when introducing event-triggered PI control are discussed in the literatures [10], [13], [16]. In [10], it is shown that event-triggering results in the sticking effect and stationary large oscillations. To overcome these two problems, [10] proposes a modified PI controller. Furthermore, [13], [16]–[18] focus on actuator saturation on event-triggered control. Actuator saturation is often observed in practical application due to physical or safety constraints.

[1]The authors are with School of Electrical Engineering and Computer Science, KTH Royal Institute of Technology, SE-100 44 Stockholm, Sweden. Emails: {takya, kallej}@kth.se
[2]Junfeng Wu is with the College of Control Science and Engineering, Zhejiang University, Hangzhou, P. R. China. Email: jfwu@zju.edu.cn

Even for linear plants, the closed-loop with actuator saturation may become unstable and stability can be guaranteed only localy [19]. Thus, it is important to consider actuator saturation for event-triggered control. In fact, the stability region is influenced by the use of event-triggered control [16]. In [16], it is shown that an anti-windup technique can significantly improve the performance of control systems with event-trigged sampling.

In this paper, we investigate event-triggered feedforward control for disturbance compensation. Especially, we consider the following scenario: i) A feedback control loop which stabilizes a plant is under operation, ii) There exists a measurable external disturbance which degrades the control performance, iii) We introduce feedforward control by measuring the disturbance through a wireless sensor. Practically, adding a new sensor into a control system under operation is often difficult since it requires installation efforts such as cabling. Hence, using wireless sensors is an effective solution [20]. When using wireless sensors, however, energy limitation affects the control performance since they have usually no reliable energy source. Thus, introducing event-triggered feedforward control is reasonable.

The contributions of this work are the following:

1) We formulate event-triggered feedforward control and derive stability conditions by using LMIs when the control input is subject to actuator saturation.
2) We also derive stability conditions of event-triggered feedforward control with anti-windup compensation.
3) We provide a numerical example which shows that the event-triggered feedforward contol significantly reduce the communication without performance degradation compared with conventional continuous-time feedforward contol.

The remainder of the paper is organized as follows. Section 2 describes the plant considered in this paper. An event-triggered feedforward contol is given in Section 3. Stability analysis under actuator saturation is provided in Section 4. Anti-windup compensation is discussed in Section 5. A numerical example is provided in Section 6. Section 7 presents the conclusion.

Notation: Throughout this paper, $\mathbb{N}$ and $\mathbb{R}$ are the sets of nonnegative integers and real numbers, respectively. A scalar variable is denoted by italic letters ($x \in \mathbb{R}$), a vector by bold italic letters ($\boldsymbol{x} \in \mathbb{R}^n$) and a matrix by upper-case bold italic letters ($\boldsymbol{X} \in \mathbb{R}^{n \times n}$). The i-th entry of a vector $\boldsymbol{x}$ is denoted by $\boldsymbol{x}_{(i)}$, and the i-th row vector of a matrix $\boldsymbol{X}$ by $\boldsymbol{X}_{(i)}$. The relation of two vectors $\boldsymbol{x} \succeq \boldsymbol{y}$ indicates $\boldsymbol{x}_{(i)} \geq \boldsymbol{y}_{(i)}$ for all elements i. The set of n by n positive definite (positive
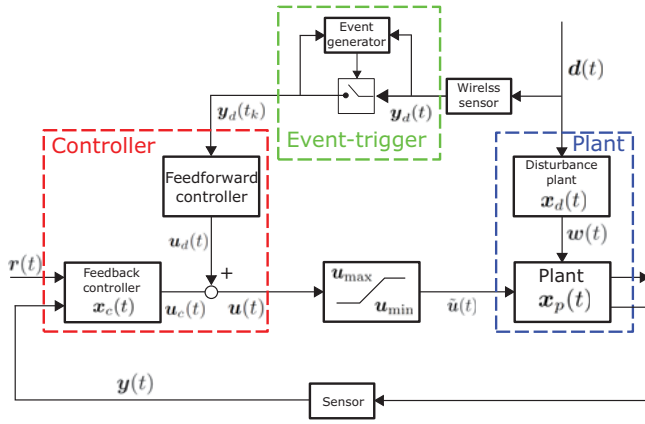
Fig. 1. Block diagram of the control system with event-triggered feedforward control

semi-definite) matrices restricted to be Hermitian over the field $\mathbb{R}^{n \times n}$ is denoted as $\mathbb{S}^n_{++}$ ($\mathbb{S}^n_+$). For simplicity, we write $\boldsymbol{X} > \boldsymbol{Y}$ ($\boldsymbol{X} \geq \boldsymbol{Y}$), where $\boldsymbol{X}, \boldsymbol{Y} \in \mathbb{S}^n_{++}$, if $\boldsymbol{X} - \boldsymbol{Y} \in \mathbb{S}^n_{++}$ ($\boldsymbol{X} - \boldsymbol{Y} \in \mathbb{S}^n_+$) and $\boldsymbol{X} > 0$ ($\boldsymbol{X} \geq 0$) if $\boldsymbol{X} \in \mathbb{S}^n_{++}$ ($\boldsymbol{X} \in \mathbb{S}^n_+$). Symmetric matrices of the form $\begin{bmatrix} \boldsymbol{A} & \boldsymbol{B}^{\mathrm{T}} \\ \boldsymbol{B} & \boldsymbol{C} \end{bmatrix}$ are written as $\begin{bmatrix} \boldsymbol{A} & \star \\ \boldsymbol{B} & \boldsymbol{C} \end{bmatrix}$ with $\boldsymbol{B}^{\mathrm{T}}$ denoting the transpose of matrix $\boldsymbol{B}$.

II. PLANT AND DISTURBANCE MODELS

In this paper, we consider event-triggered feedforward control compensating an external disturbance as depicted in Figure 1. The plant is given by a continuous-time linear system

$$\dot{\boldsymbol{x}}_p(t) = \tilde{\boldsymbol{A}}\boldsymbol{x}_p(t) + \tilde{\boldsymbol{B}}\tilde{\boldsymbol{u}}(t) + \tilde{\boldsymbol{B}}_w \boldsymbol{w}(t), \quad \boldsymbol{x}_p(0) = \boldsymbol{x}_{p0} \quad (1)$$

$$\boldsymbol{y}(t) = \tilde{\boldsymbol{C}}\boldsymbol{x}_p(t) \quad (2)$$

where $\boldsymbol{x}_p \in \mathbb{R}^{n_p}$ denotes the state, $\tilde{\boldsymbol{u}} \in \mathbb{R}^m$ control, $\boldsymbol{w} \in \mathbb{R}^p$ disturbance, and $\boldsymbol{y} \in \mathbb{R}^q$ the measurement output. The disturbance affects the plant state through the linear disturbance system

$$\dot{\boldsymbol{x}}_d(t) = \tilde{\boldsymbol{A}}_d \boldsymbol{x}_d(t) + \tilde{\boldsymbol{B}}_d \boldsymbol{d}(t), \quad \boldsymbol{x}_d(0) = \boldsymbol{x}_{d0} \quad (3)$$

$$\boldsymbol{w}(t) = \tilde{\boldsymbol{C}}_w \boldsymbol{x}_d(t) \quad (4)$$

where $\boldsymbol{x}_d \in \mathbb{R}^{n_d}$ denotes the disturbance state, $\boldsymbol{d} \in \mathbb{R}^r$ the original disturbance, which is assumed to be continuous in t and bounded according to

$$\boldsymbol{d} \in \mathcal{V}_D = \left\{ \boldsymbol{d} \in \mathbb{R}^r : \boldsymbol{d}^{\mathrm{T}} \boldsymbol{Q}_D \boldsymbol{d} \leq \epsilon_D^{-1} \right\} \quad (5)$$

with $\boldsymbol{Q}_D \in \mathbb{S}^r_{++}$ and $\epsilon_D > 0$. The matrices $\tilde{\boldsymbol{A}}$, $\tilde{\boldsymbol{B}}$, $\tilde{\boldsymbol{B}}_w$, $\tilde{\boldsymbol{C}}$, $\tilde{\boldsymbol{A}}_d$, $\tilde{\boldsymbol{B}}_d$, and $\tilde{\boldsymbol{C}}_w$ are real matrices of appropriate dimensions. In the following, for the plant (1)–(2), we assume that $(\tilde{\boldsymbol{A}}, \tilde{\boldsymbol{B}})$ is controllable and $(\tilde{\boldsymbol{A}}, \tilde{\boldsymbol{C}})$ is observable. To ensure the boundedness of $\boldsymbol{w}(t)$, we also need to assume that the disturbance system (3)–(4) is stable, i.e., $\tilde{\boldsymbol{A}}_d$ is Hurwitz.

The plant input $\tilde{\boldsymbol{u}}(t)$ is given by $\tilde{\boldsymbol{u}}(t) = \mathbf{sat}(\boldsymbol{u}(t))$, where $\mathbf{sat}(\cdot)$ denotes the saturation function

$$\mathbf{sat}(\boldsymbol{u})_{(i)} = \begin{cases} \boldsymbol{u}_{\max(i)}, & \text{if } \boldsymbol{u}_{(i)} > \boldsymbol{u}_{\max(i)}; \\ \boldsymbol{u}_{(i)}, & \text{if } -\boldsymbol{u}_{\min(i)} \leq \boldsymbol{u}_{(i)} \leq \boldsymbol{u}_{\max(i)}; \\ -\boldsymbol{u}_{\min(i)}, & \text{if } \boldsymbol{u}_{(i)} < -\boldsymbol{u}_{\min(i)}, \end{cases} \quad (6)$$

with $i \in \{1, \ldots, m\}$, where $\boldsymbol{u}_{\max} \succeq 0$ and $\boldsymbol{u}_{\min} \succeq 0$ are the upper and lower bound vectors of the input $\tilde{\boldsymbol{u}}$, respectively. For simplicity, we assume symmetric constraints $\boldsymbol{u}_0 = \boldsymbol{u}_{\max} = \boldsymbol{u}_{\min}$.

III. FEEDBACK CONTROL AND EVENT-TRIGGERED FEEDFORWARD CONTROL

The goal of this paper is to investigate event-triggered feedforward control when applied to a feedback control system already under operation. See Figure 1. We assume that the feedback control is established with continuous-time information exchanged through wired communication.

A. Feedback controller

In the following we consider a general linear dynamic output feedback controller given by

$$\dot{\boldsymbol{x}}_c(t) = \tilde{\boldsymbol{A}}_c \boldsymbol{x}_c(t) + \tilde{\boldsymbol{B}}_c \boldsymbol{y}(t) + \tilde{\boldsymbol{B}}_{cR} \boldsymbol{r}(t), \quad \boldsymbol{x}_c(0) = \boldsymbol{x}_{c0} \quad (7)$$

$$\boldsymbol{u}_c(t) = \tilde{\boldsymbol{C}}_c \boldsymbol{x}_c(t) + \tilde{\boldsymbol{D}}_c \boldsymbol{y}(t) + \tilde{\boldsymbol{D}}_{cR} \boldsymbol{r}(t) \quad (8)$$

where $\boldsymbol{x}_c \in \mathbb{R}^{n_c}$ denotes the state, $\boldsymbol{u}_c \in \mathbb{R}^m$ feedback control, and $\boldsymbol{r} \in \mathbb{R}^s$ reference signal. The matrices $\tilde{\boldsymbol{A}}_c$, $\tilde{\boldsymbol{B}}_c$, $\tilde{\boldsymbol{B}}_{cR}$, $\tilde{\boldsymbol{C}}_c$, $\tilde{\boldsymbol{D}}_c$, and $\tilde{\boldsymbol{D}}_{cR}$ are real matrices of appropriate dimensions.

B. Feedforward controller

We assume that the disturbance considered can be observed by an event-triggered wireless sensor which is described as

$$\boldsymbol{y}_d(t) = \tilde{\boldsymbol{C}}_d \boldsymbol{d}(t) \quad (9)$$

where $\boldsymbol{y}_d \in \mathbb{R}^{m_d}$ is the original disturbance measurement output and $\tilde{\boldsymbol{C}}_d$ is a real matrix with appropriate dimension. Based on the measurement $\boldsymbol{y}_d(t)$, a wireless sensor invokes a new communication event. Let t_k with $k \in \mathbb{N}$ be the time of transmission k. Then the new event occurs whenever the disturbance error $\boldsymbol{e}(t)$ given by

$$\boldsymbol{e}(t) = \boldsymbol{y}_d(t) - \boldsymbol{y}_d(t_k), \quad \forall t \in [t_k, t_{k+1}) \quad (10)$$

reaches the boundary of the set

$$\mathcal{W} = \left\{ \boldsymbol{e} \in \mathbb{R}^{m_d} : \boldsymbol{e}^{\mathrm{T}} \boldsymbol{R} \boldsymbol{e} \leq \delta^{-1} \right\} \quad (11)$$

with $\boldsymbol{R} \in \mathbb{S}^{n_d}_{++}$ and $\delta > 0$, that is, when $\boldsymbol{e}(t) \in \partial \mathcal{W}$.

The feedforward controller calculates the output $\boldsymbol{u}_d(t) \in \mathbb{R}^m$ based on the disturbance information form the wireless sensor. We consider static feedforward control described as

$$\boldsymbol{u}_d(t) = \tilde{\boldsymbol{D}}_{cD} \boldsymbol{y}_d(t_k), \quad \forall t \in [t_k, t_{k+1}), \quad (12)$$

which compensates the control vector by

$$\boldsymbol{u}(t) = \boldsymbol{u}_c(t) + \boldsymbol{u}_d(t). \quad (13)$$

C. Closed-loop system

From (1)–(4), (7)–(8), (10)–(12), and (13), and by introducing the augmented state vector

$$\boldsymbol{x}(t) = \begin{bmatrix} \boldsymbol{x}_p(t) \\ \boldsymbol{x}_c(t) \\ \boldsymbol{x}_d(t) \end{bmatrix} \in \mathbb{R}^n$$

where $n = n_p + n_c + n_d$, we obtain the augmented state-space model

$$\dot{\boldsymbol{x}}(t) = \boldsymbol{A}\boldsymbol{x}(t) + \boldsymbol{B}\tilde{\boldsymbol{u}}(t) + \boldsymbol{B}_D\boldsymbol{d}(t) + \boldsymbol{B}_R\boldsymbol{r}(t) \quad (14)$$

$$\boldsymbol{u}(t) = \boldsymbol{K}\boldsymbol{x}(t) + \boldsymbol{K}_D\boldsymbol{d}(t) + \boldsymbol{K}_E\boldsymbol{e}(t) + \boldsymbol{K}_R\boldsymbol{r}(t) \quad (15)$$

$$\boldsymbol{y}(t) = \boldsymbol{C}\boldsymbol{x}(t) \quad (16)$$

with

$$\boldsymbol{A} = \begin{bmatrix} \tilde{\boldsymbol{A}} & \boldsymbol{O} & \tilde{\boldsymbol{B}}_w\tilde{\boldsymbol{C}}_w \\ \tilde{\boldsymbol{B}}_c\tilde{\boldsymbol{C}} & \tilde{\boldsymbol{A}}_c & \boldsymbol{O} \\ \boldsymbol{O} & \boldsymbol{O} & \tilde{\boldsymbol{A}}_d \end{bmatrix}, \quad \boldsymbol{B} = \begin{bmatrix} \tilde{\boldsymbol{B}} \\ \boldsymbol{O} \\ \boldsymbol{O} \end{bmatrix},$$

$$\boldsymbol{B}_D = \begin{bmatrix} \boldsymbol{O} \\ \boldsymbol{O} \\ \tilde{\boldsymbol{B}}_d \end{bmatrix}, \quad \boldsymbol{B}_R = \begin{bmatrix} \boldsymbol{O} \\ \tilde{\boldsymbol{B}}_{cR} \\ \boldsymbol{O} \end{bmatrix},$$

$$\boldsymbol{K} = \begin{bmatrix} \tilde{\boldsymbol{D}}_c\tilde{\boldsymbol{C}} & \tilde{\boldsymbol{C}}_c & \boldsymbol{O} \end{bmatrix}, \quad \boldsymbol{K}_D = \tilde{\boldsymbol{D}}_{cD}\tilde{\boldsymbol{C}}_d, \quad \boldsymbol{K}_E = -\tilde{\boldsymbol{D}}_{cD},$$

$$\boldsymbol{K}_R = \tilde{\boldsymbol{D}}_{cR}, \quad \boldsymbol{C} = \begin{bmatrix} \tilde{\boldsymbol{C}} & \boldsymbol{O} & \boldsymbol{O} \end{bmatrix}.$$

To characterize the stability of the closed-loop system (14)–(16), we first introduce the deadzone nonlinearity [19], which is defined by

$$\phi(\boldsymbol{u}) = \mathbf{sat}(\boldsymbol{u}) - \boldsymbol{u}. \quad (17)$$

The deadzone nonlinearity allows us to use a modified sector condition as follows.

Lemma 1: [19] If $\boldsymbol{v} \in \mathbb{R}^m$ and $\boldsymbol{z} \in \mathbb{R}^m$ are elements of the set

$$\mathcal{S} = \left\{ \boldsymbol{v}, \boldsymbol{z} \in \mathbb{R}^m : |\boldsymbol{v}_{(i)} - \boldsymbol{z}_{(i)}| \le \boldsymbol{u}_{0(i)}, \ \forall i \in \{1, \ldots, m\} \right\}$$

then the nonlinearity $\phi(\boldsymbol{v})$ satisfies the inequality

$$\phi(\boldsymbol{v})^{\mathrm{T}}\boldsymbol{T}(\phi(\boldsymbol{v}) + \boldsymbol{z}) \le 0$$

for any diagonal matrix $\boldsymbol{T} \in \mathbb{S}_{++}$.

By using (17), we can rewrite the closed-loop system as

$$\dot{\boldsymbol{x}}(t) = (\boldsymbol{A} + \boldsymbol{B}\boldsymbol{K})\boldsymbol{x}(t)$$
$$+ \bar{\boldsymbol{B}}\phi(\boldsymbol{K}\boldsymbol{x}(t) + \boldsymbol{K}_D\boldsymbol{d}(t) + \boldsymbol{K}_E\boldsymbol{e}(t) + \boldsymbol{K}_R\boldsymbol{r}(t))$$
$$+ (\boldsymbol{B}_D + \boldsymbol{B}\boldsymbol{K}_D)\boldsymbol{d}(t) + \boldsymbol{B}\boldsymbol{K}_E\boldsymbol{e}(t)$$
$$+ (\boldsymbol{B}_R + \boldsymbol{B}\boldsymbol{K}_R)\boldsymbol{r}(t) \quad (18)$$

$$\boldsymbol{y}(t) = \boldsymbol{C}\boldsymbol{x}(t). \quad (19)$$

where $\bar{\boldsymbol{A}} = \boldsymbol{A} + \boldsymbol{B}\boldsymbol{K}$ and $\bar{\boldsymbol{B}} = \boldsymbol{B}$. Note that the feedback controller (7)–(8) can stabilize the plant (1)–(2) at least for a sufficiently small region around the equilibrium point of the system (18). Thus, the matrix $\bar{\boldsymbol{A}}$ is Hurwitz. The closed-loop system is illustrated in Figure 2. For simplicity, we assume that $\boldsymbol{r}(t) \equiv 0$ in the following.
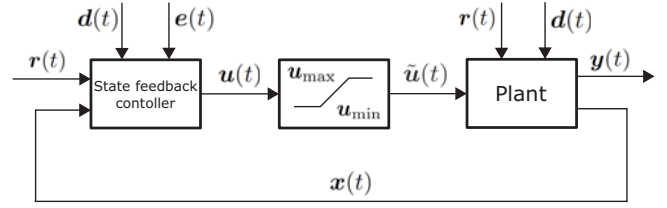

Fig. 2. Block diagram of the closedd-loop system with event-triggered feedforward control

IV. STABILITY ANALYSIS UNDER ACTUATOR SATURATION

For practical application, it is important to consider input constraints since almost all systems have physical or safety constraints. Under actuator saturation, the stability is guaranteed only locally. Hence, our stability analysis focuses on estimating the stability region.

First, we derive stability conditions of the system with continuous-time feedforward control, which is simple extension of the discussion in [19]. It is used later to evaluate the effect of the event-triggered feedforward control. With continuous-time feedforward control, the closed-loop system (18)–(19) can be rewritten as

$$\dot{\boldsymbol{x}}(t) = \bar{\boldsymbol{A}}\boldsymbol{x}(t) + \bar{\boldsymbol{B}}\phi(\boldsymbol{K}\boldsymbol{x}(t) + \boldsymbol{K}_D\boldsymbol{d}(t)$$
$$+ (\boldsymbol{B}_D + \boldsymbol{B}\boldsymbol{K}_D)\boldsymbol{d}(t) \quad (20)$$

$$\boldsymbol{y}(t) = \boldsymbol{C}\boldsymbol{x}(t). \quad (21)$$

Then we have the following theorem.

Theorem 2: If there exist a symmetric matrix $\boldsymbol{W} \in \mathbb{S}_{++}^n$, a diagonal matrix $\boldsymbol{S} \in \mathbb{S}_{++}^m$, a matrix $\boldsymbol{Z} \in \mathbb{R}^{m \times n}$, three positive scalars τ_1, τ_2 and η satisfying

$$\begin{bmatrix} \boldsymbol{W}\bar{\boldsymbol{A}}^{\mathrm{T}} + \bar{\boldsymbol{A}}\boldsymbol{W} + \tau_1\boldsymbol{W} & \star & \star \\ \boldsymbol{S}\bar{\boldsymbol{B}}^{\mathrm{T}} - \boldsymbol{Z} - \boldsymbol{K}\boldsymbol{W} & -2\boldsymbol{S} & \star \\ (\boldsymbol{B}_D + \boldsymbol{B}\boldsymbol{K}_D)^{\mathrm{T}} & -\boldsymbol{K}_D^{\mathrm{T}} & -\tau_2\boldsymbol{Q}_D \end{bmatrix} < 0 \quad (22)$$

$$\begin{bmatrix} \boldsymbol{W} & \boldsymbol{Z}_{(i)}^{\mathrm{T}} \\ \boldsymbol{Z}_{(i)} & \eta\boldsymbol{u}_{0(i)}^2 \end{bmatrix} \ge 0, \quad i = 1, \ldots, m \quad (23)$$

$$-\tau_1\epsilon_D + \tau_2\eta < 0 \quad (24)$$

then for any $\boldsymbol{d} \in \mathcal{V}_D$ and $\boldsymbol{x}(0) \in \mathcal{E}(\boldsymbol{P}, \eta)$ with $\boldsymbol{P} = \boldsymbol{W}^{-1}$, the state $\boldsymbol{x}(t)$ of closed-loop system (20)–(21) does not leave the ellipsoid $\mathcal{E}(\boldsymbol{P}, \eta)$ for all $t \ge 0$.

Proof: It follows from Remark 3.1 and Proposition 3.6 in [19]. ∎

Remark 3: It is obvious that the stability conditions of the system without feedforward control can be derived by substituting $\boldsymbol{K}_D = \boldsymbol{O}$ which corresponds Proposition 3.6 in [19].

Next, we derive stability conditions for event-triggered feedforward control systems.

Theorem 4: If there exist a symmetric matrix $\boldsymbol{W} \in \mathbb{S}_{++}^n$, a diagonal matrix $\boldsymbol{S} \in \mathbb{S}_{++}^m$, a matrix $\boldsymbol{Z} \in \mathbb{R}^{m \times n}$, four

positive scalars τ_1, τ_2, τ_3 and η satisfying

$$
\begin{bmatrix}
\boldsymbol{W}\bar{\boldsymbol{A}}^\mathrm{T} + \bar{\boldsymbol{A}}\boldsymbol{W} + \tau_1\boldsymbol{W} & \star & \star & \star \\
\boldsymbol{S}\bar{\boldsymbol{B}}^\mathrm{T} - \boldsymbol{Z} - \boldsymbol{K}\boldsymbol{W} & -2\boldsymbol{S} & \star & \star \\
(\boldsymbol{B}_D + \boldsymbol{B}\boldsymbol{K}_D)^\mathrm{T} & -\boldsymbol{K}_D^\mathrm{T} & -\tau_2\boldsymbol{Q}_D & \star \\
\boldsymbol{K}_E^\mathrm{T}\boldsymbol{B}^\mathrm{T} & -\boldsymbol{K}_E^\mathrm{T} & \boldsymbol{O} & -\tau_3\boldsymbol{R}
\end{bmatrix} < 0
\tag{25}
$$

$$
\begin{bmatrix}
\boldsymbol{W} & \boldsymbol{Z}_{(i)}^\mathrm{T} \\
\boldsymbol{Z}_{(i)} & \eta\boldsymbol{u}_{0(i)}^2
\end{bmatrix} \geq 0, \quad i = 1,\ldots,m
\tag{26}
$$

$$
-\tau_1\delta\epsilon_D + \tau_2\delta\eta + \tau_3\epsilon_D\eta < 0
\tag{27}
$$

then for any $\boldsymbol{d} \in \mathcal{V}_D$, $\boldsymbol{e} \in \mathcal{W}$ and $\boldsymbol{x}(0) \in \mathcal{E}(\boldsymbol{P},\eta)$ with $\boldsymbol{P} = \boldsymbol{W}^{-1}$, the state $\boldsymbol{x}(t)$ of closed-loop system (18)–(19) does not leave the ellipsoid $\mathcal{E}(\boldsymbol{P},\eta)$ for all $t \geq 0$.

Proof: By setting $\boldsymbol{v} = \boldsymbol{u} = \boldsymbol{K}\boldsymbol{x} + \boldsymbol{K}_D\boldsymbol{d} + \boldsymbol{K}_E\boldsymbol{e}$ and $\boldsymbol{z} = \boldsymbol{u} + \boldsymbol{G}\boldsymbol{x} = \boldsymbol{K}\boldsymbol{x} + \boldsymbol{K}_D\boldsymbol{d} + \boldsymbol{K}_E\boldsymbol{e} + \boldsymbol{G}\boldsymbol{x}$, Lemma 1 guarantees that

$$
\phi^\mathrm{T}(\boldsymbol{u})\boldsymbol{T}(\phi(\boldsymbol{u}) + \boldsymbol{u} + \boldsymbol{G}\boldsymbol{x}) \leq 0
\tag{28}
$$

for any $\boldsymbol{x}$ belonging to the set

$$
\mathcal{S}_{\boldsymbol{G}} = \{\boldsymbol{x} \in \mathbb{R}^n : |\boldsymbol{G}_{(i)}\boldsymbol{x}| \leq \boldsymbol{u}_{0(i)}, \forall i\}.
$$

Consider Lyapunov function candidate

$$
V(\boldsymbol{x}) = \boldsymbol{x}^\mathrm{T}\boldsymbol{P}\boldsymbol{x}
$$

with $\boldsymbol{P} = \boldsymbol{P}^\mathrm{T} > 0$, which defines the ellipsoid $\mathcal{E}(\boldsymbol{P},\eta)$. This ellipsoid is included in the set $\mathcal{S}_{\boldsymbol{G}}$ if the condition (26) is satisfied. This can be shown by left-multiplying the vector $[\eta\boldsymbol{u}_{0(i)}(\boldsymbol{W}^{-1}\boldsymbol{x})^\mathrm{T} \quad \pm 1]$ and right-multiplying $[\eta\boldsymbol{u}_{0(i)}(\boldsymbol{W}^{-1}\boldsymbol{x})^\mathrm{T} \pm 1]^\mathrm{T}$ by the matrix in the condition (26).

Next, we will show that $\dot{V}(\boldsymbol{x}) < 0$ for any $\boldsymbol{x} \in \mathrm{int}\mathcal{E}(\boldsymbol{P},\eta)$ and $\boldsymbol{d} \in \mathcal{V}_D$, $\boldsymbol{e} \in \mathcal{W}$ so that any trajectories of $\boldsymbol{x}(t)$ never leave the ellipsoid $\mathcal{E}(\boldsymbol{P},\eta)$. By applying the S-procedure, we have the condition

$$
\dot{V}(\boldsymbol{x}) + \tau_1(\boldsymbol{x}^\mathrm{T}\boldsymbol{P}\boldsymbol{x} - \eta^{-1}) + \tau_2(\epsilon_D^{-1} - \boldsymbol{d}^\mathrm{T}\boldsymbol{Q}_D\boldsymbol{d}) + \\
\tau_3(\delta^{-1} - \boldsymbol{e}^\mathrm{T}\boldsymbol{R}\boldsymbol{e}) < 0,
$$

which can be split further into two conditions:

$$
\dot{V}(\boldsymbol{x}) + \tau_1\boldsymbol{x}^\mathrm{T}\boldsymbol{P}\boldsymbol{x} - \tau_2\boldsymbol{d}^\mathrm{T}\boldsymbol{Q}_D\boldsymbol{d} - \tau_3\boldsymbol{e}^\mathrm{T}\boldsymbol{R}\boldsymbol{e} < 0 \\
-\tau_1\eta^{-1} + \tau_2\epsilon_D^{-1} + \tau_3\delta^{-1} < 0.
$$

The condition (27) directly results in the second inequality above. By the inequality (28), we have

$$
\dot{V}(\boldsymbol{x}) + \tau_1\boldsymbol{x}^\mathrm{T}\boldsymbol{P}\boldsymbol{x} - \tau_2\boldsymbol{d}^\mathrm{T}\boldsymbol{Q}_D\boldsymbol{d} - \tau_3\boldsymbol{e}^\mathrm{T}\boldsymbol{R}\boldsymbol{e} \\
\leq \dot{V}(\boldsymbol{x}) + \tau_1\boldsymbol{x}^\mathrm{T}\boldsymbol{P}\boldsymbol{x} - \tau_2\boldsymbol{d}^\mathrm{T}\boldsymbol{Q}_D\boldsymbol{d} - \tau_3\boldsymbol{e}^\mathrm{T}\boldsymbol{R}\boldsymbol{e} \\
- 2\phi^\mathrm{T}\boldsymbol{T}(\phi + \boldsymbol{u} + \boldsymbol{G}\boldsymbol{x}).
$$

By using the system representation (14) and transformation $\boldsymbol{W} = \boldsymbol{P}^{-1}$, $\boldsymbol{S} = \boldsymbol{T}^{-1}$ and $\boldsymbol{Z} = \boldsymbol{G}\boldsymbol{W}$, the condition (25) guarantees that the right term of the above inequality is negative, which can be shown by left-multiplying $[(\boldsymbol{W}^{-1}\boldsymbol{x})^\mathrm{T} \quad (\boldsymbol{S}^{-1}\phi)^\mathrm{T} \quad \boldsymbol{d}^\mathrm{T} \quad \boldsymbol{e}^\mathrm{T}]$ and right-multiplying $[(\boldsymbol{W}^{-1}\boldsymbol{x})^\mathrm{T} \quad (\boldsymbol{S}^{-1}\phi)^\mathrm{T} \quad \boldsymbol{d}^\mathrm{T} \quad \boldsymbol{e}^\mathrm{T}]^\mathrm{T}$ by the matrix in the condition (25). This completes the proof. ∎

V. ANTI-WINDUP COMPENSATION

It is known that anti-windup is effective to compensate performance degradation due to actuator saturation [16], [19]. In this section, we define the stability conditions for event-triggered feedforward control with anti-windup compensation. The idea of anti-windup compensation is to feed back the difference between control input and actual actuator output, i.e., $\phi(\boldsymbol{u})$, to the controller. We assume that the anti-windup feedback gain is static $\boldsymbol{K}_{AW}$, then the controller state is given by

$$
\dot{\boldsymbol{x}}_c(t) = \tilde{\boldsymbol{A}}_c\boldsymbol{x}_c(t) + \tilde{\boldsymbol{B}}_c\boldsymbol{y}(t) + \boldsymbol{K}_{AW}\phi(\boldsymbol{u}), \quad \boldsymbol{x}_c(0) = \boldsymbol{x}_{c0},
$$

and therefore, the closed loop system becomes

$$
\dot{\boldsymbol{x}}(t) = \bar{\boldsymbol{A}}\boldsymbol{x}(t) + \boldsymbol{B}_{AW}\phi(\boldsymbol{K}\boldsymbol{x}(t) + \boldsymbol{K}_D\boldsymbol{d}(t) + \boldsymbol{K}_E\boldsymbol{e}(t)) \\
+ (\boldsymbol{B}_D + \boldsymbol{B}\boldsymbol{K}_D)\boldsymbol{d}(t) + \boldsymbol{B}\boldsymbol{K}_E\boldsymbol{e}(t)
\tag{29}
$$

$$
\boldsymbol{y}(t) = \boldsymbol{C}\boldsymbol{x}(t).
\tag{30}
$$

with

$$
\boldsymbol{B}_{AW} = \begin{bmatrix} \tilde{\boldsymbol{B}} \\ \boldsymbol{K}_{AW} \\ \boldsymbol{O} \end{bmatrix}.
$$

Now, we have the following stability conditions which is obtained by replacing $\bar{\boldsymbol{B}}$ by $\boldsymbol{B}_{AW}$ in Theorem 4.

Corollary 5: If there exist a symmetric matrix $\boldsymbol{W} \in \mathbb{S}_{++}^n$, a diagonal matrix $\boldsymbol{S} \in \mathbb{S}_{++}^m$, a matrix $\boldsymbol{Z} \in \mathbb{R}^{m \times n}$, four positive scalars τ_1, τ_2, τ_3 and η satisfying

$$
\begin{bmatrix}
\boldsymbol{W}\bar{\boldsymbol{A}}^\mathrm{T} + \bar{\boldsymbol{A}}\boldsymbol{W} + \tau_1\boldsymbol{W} & \star & \star & \star \\
\boldsymbol{S}\boldsymbol{B}_{AW}^\mathrm{T} - \boldsymbol{Z} - \boldsymbol{K}\boldsymbol{W} & -2\boldsymbol{S} & \star & \star \\
(\boldsymbol{B}_D + \boldsymbol{B}\boldsymbol{K}_D)^\mathrm{T} & -\boldsymbol{K}_D^\mathrm{T} & -\tau_2\boldsymbol{Q}_D & \star \\
\boldsymbol{K}_E^\mathrm{T}\boldsymbol{B}^\mathrm{T} & -\boldsymbol{K}_E^\mathrm{T} & \boldsymbol{O} & -\tau_3\boldsymbol{R}
\end{bmatrix} < 0
\tag{31}
$$

$$
\begin{bmatrix}
\boldsymbol{W} & \boldsymbol{Z}_{(i)}^\mathrm{T} \\
\boldsymbol{Z}_{(i)} & \eta\boldsymbol{u}_{0(i)}^2
\end{bmatrix} \geq 0, \quad i = 1,\ldots,m
\tag{32}
$$

$$
-\tau_1\delta\epsilon_D + \tau_2\delta\eta + \tau_3\epsilon_D\eta < 0
\tag{33}
$$

then for any $\boldsymbol{d} \in \mathcal{V}_D$, $\boldsymbol{e} \in \mathcal{W}$ and $\boldsymbol{x}(0) \in \mathcal{E}(\boldsymbol{P},\eta)$ with $\boldsymbol{P} = \boldsymbol{W}^{-1}$, the state $\boldsymbol{x}(t)$ of closed-loop system (29)–(30) does not leave the ellipsoid $\mathcal{E}(\boldsymbol{P},\eta)$ for all $t \geq 0$.

VI. NUMERICAL EXAMPLE

In this section, we provide a numerical example of scalar PI control to see the effect of event-triggered feedforward control.

A. Plant and controller

Consider the following scalar unstable system

$$
\dot{x}_p(t) = 0.5x_p(t) + \tilde{u}(t) + 2x_d(t), \quad x(0) = 0 \\
y(t) = x_p(t)
$$

and the disturbance system

$$
\dot{x}_d(t) = -3x_d(t) + 2d(t), \quad x_d(0) = 0 \\
w(t) = x_d(t) \\
y_d(t) = d(t_k), \ t \in [t_k, t_{k+1})
$$

with PI control including feedforward compensation

$$\dot{x}_c(t) = -y(t)$$
$$u(t) = x_c(t) - 1.2y(t) + k_f y_d(t)$$

where k_f is the scalar feedfoward gain. The input is affected by the actuator saturation

$$\tilde{u}(t) = \mathrm{sat}(u(t)) = \begin{cases} 2, & \text{if } u(t) > 2; \\ u(t), & \text{if } -2 \le u(t) \le 2; \\ -2, & \text{if } u(t) < -2. \end{cases}$$

An event is generated whenever $e^2(t) = \delta^{-1}$, i.e., $\boldsymbol{R} = 1$. We define $\bar{e} \triangleq \delta^{-1/2}$ for simplicity.

B. Computation of stability region

In the simulation, we evaluate the region of stability $\mathcal{E}(\boldsymbol{P}, \eta)$ for some cases. To estimate the region, we formulate the following optimization problem with different constraints corresponding to the three cases in Sections 4 and 5:

$$\begin{aligned} \min \quad & \mathrm{trace}(-\boldsymbol{W}) \\ \text{s.t.} \quad & (22)\text{–}(24), \text{ or} \\ & (25)\text{–}(27), \text{ or} \\ & (31)\text{–}(33). \end{aligned}$$

With this objective function, the optimization problem is a semi-definite program under given τ_i, $i = 1, 2, 3$, which is effectively solved by YALMIP toolbox [21]. Note that the outcome of the optimization problem depends on the values of τ_i. Thus, a search on a grid defined by τ_i is needed in order to obtain the maximum stability region [19].

Figure 3 shows the stability regions of x_p and x_c derived based on Theorem 2 and Theorem 4 for the three cases: (i) event-triggered feedforward control (ET-FF: red) with $\bar{e} = 0.1$ and $k_f = -0.75$, (ii) continuous-time feedforward control (CT-FF: green) with $k_f = -0.75$, and (iii) no feedforward control (no-FF: blue) with $k_f = 0$. We find that the continuous-time feedforward control obtains the largest stability region and PI control without feedfoward control does the smallest. The event-triggered feedforward control has smaller stability region than continuous-time one. The difference of the stability regions with the continuous-time feedforward control stems from the disturbance measurement error $\boldsymbol{e}(t)$. However, even if the information of disturbance is thinned out by event-generator, the event-triggered feedforward control still has larger stability region compared with the case without feedforward control. In addition, comparing two event-triggering conditions with $\bar{e} = 0.1$ and $\bar{e} = 0.3$, the case with $\bar{e} = 0.1$ has larger stability region. This is due to smaller disturbance error $e(t)$ than the case with $\bar{e} = 0.3$. We also compare the two cases: event-triggered feedforward control with and without anti-windup compensation. The result with $k_{AW} = -1$ is shown in Figure 4. We find that anti-windup compensation has much influence on the size of the stability region for event-triggered feedforward control.
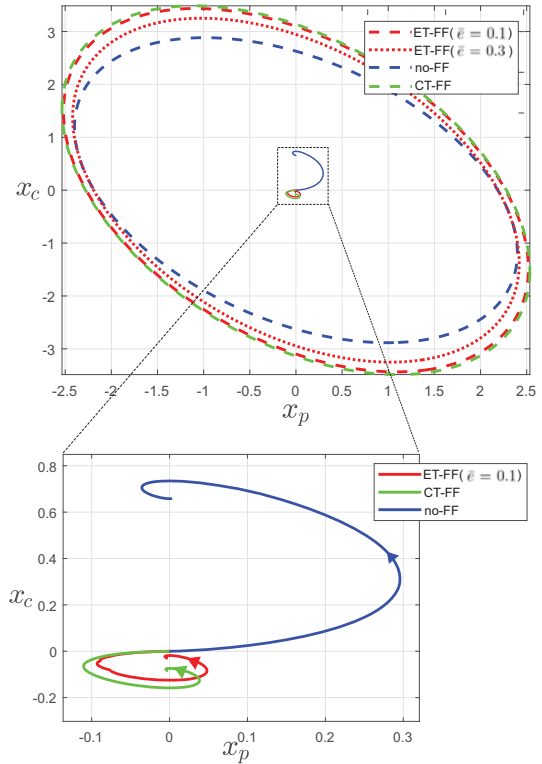

Fig. 3. Stability regions (dashed line, dotted lines) and the trajectories (solid lines) with the disturbance (34) of three cases: (i) event-triggered feedforward control (red, ET-FF), (ii) continuous-time feedforward control (green, CT-FF), and (iii) no feedforward control (blue, no-FF)
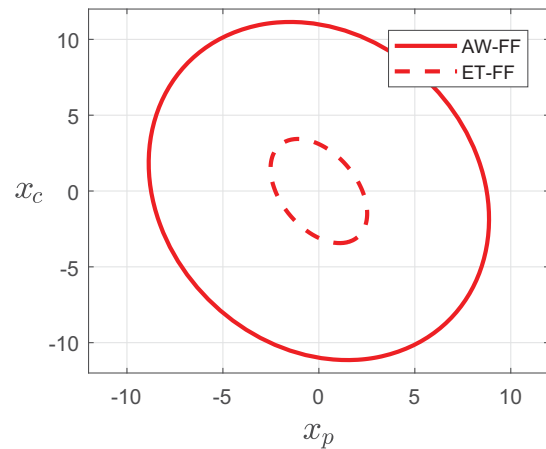

Fig. 4. Stability regions of event-triggered feedforward control: (i) with anti-windup compensation (solid line, AWET-FF), (ii) without anti-windup compensation (dashed line, ET-FF)
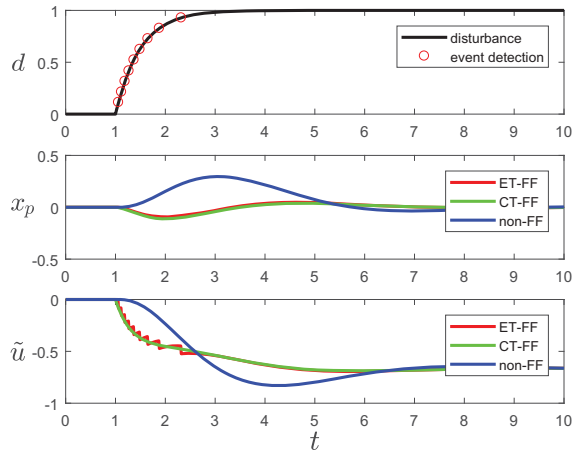
Fig. 5. Top: Disturbance and triggering times. Middle: Outputs of three cases; (i) with event-triggered feedforward control (red), (ii) with continuous-time feedworward control (green), and (iii) no feedforward control (blue). Bottom: Inputs of the same three cases.

C. Behaviours of the control loop

We also show the behaviours of each control loop with a given disturbance. Here, we assume that a disturbance appears when $t = 1$ [s] with

$$d(t) = 1 - e^{-0.5(t+1)}. \tag{34}$$

The results of the three cases: (i) PI control with event-triggered feedforward control (ET-FF: red) with $\bar{e} = 0.1$ and $k_f = -0.75$, (ii) PI control with continuous-time feedforward control (CT-FF, green) with $k_f = -0.75$, and (iii) PI control without feedforward control (no-FF, blue), are shown in Figures 3 and 5. From Figure 5, we find that the event-triggered feedfoward control achieves almost the same performance against the disturbance as the continuous-time feedforward control with only 9 samples of the disturbance being communicated. This implies that the event-triggered feedforward control significantly reduces the communication with basically no performance degradation compared with the continuous-time feedforward control. In Figure 3, the trajectories of the three cases converge to different equilibrium points. This difference comes from the feedforward gain k_f, and leads to the performance improvement.

VII. Conclusion

In this paper, we investigated event-triggered feedforward control under actuator saturation. As a main result, LMI conditions were derived to determine the stability region of the control loop with event-trigged feedforward control. The numerical example showed that event-triggered feedforward control is able to significantly reduce the communication with no performance degradation compared with continuous-time feedfoward control. Possible future works will focus on systematic design synthesis to determine the feedforward gain.

References

[1] D. E. Seborg, D. A. Mellichamp, T. F. Edgar, and F. J. Doyle III, *Process Dynamics and Control*. John Wiley & Sons, 2010.

[2] K. J. Åström and T. Hägglund, *Advanced PID Control*. International Society of Automation, 2006.

[3] Y. Hamada, "Preview feedforward compensation: LMI synthesis and flight simulation," in *Proc. of the 20th IFAC Symposium of Automatic Control in Aerospace*, 2016, pp. 397–402.

[4] P. Li, J. Lam, and K. C. Cheung, "Multi-objective control for active vehicle suspension with wheelbase preview," *J. of Sound and Vibration*, vol. 333, no. 21, pp. 5269–5282, 2014.

[5] P. Tabuada, "Event-triggered real-time scheduling of stabilizing control tasks," *IEEE Transactions on Automatic Control*, vol. 52, no. 9, pp. 1680–1685, 2007.

[6] W. Heemels, J. Sandee, and P. van den Bosch, "Analysis of event-driven controllers for linear systems," *Int. J. of Control*, vol. 81, no. 4, pp. 571–590, 2008.

[7] T. Blevins, D. Chen, M. Nixon, and W. Wojsznis, *Wireless Control Foundation: Continuous and Discrete Control for the Process Industry*. International Society of Automation, 2015.

[8] K.-E. Årzén, "A simple event-based PID controller," in *Proc. of 14th IFAC World Congress*, vol. 18, 1999, pp. 423–428.

[9] S. Reimann, W. Wu, and S. Liu, "PI control and scheduling design for embedded control systems," in *Proc. of the 19th IFAC World Congress*, 2014, pp. 11 111–11 116.

[10] U. Tiberi, J. Araújo, and K. H. Johansson, "On event-based PI control of first-order processes," in *Proc. of the 2nd IFAC Conf. on Advances in PID Control*, 2012.

[11] M. Rabi and K. H. Johansson, "Event-triggered strategies for industrial control over wireless networks," in *Proc. of the 4th Int. Conf. on Wireless Internet*, 2008, pp. 1–7.

[12] S. Reimann, D. H. Van, S. Al-Areqi, and S. Liu, "Stability analysis and PI control synthesis under event-triggered communication," in *Proc. of the 14th European Control Conf.*, 2015, pp. 2174–2179.

[13] L. Moreira, L. Groff, J. G. da Silva, and S. Tarbouriech, "Event-triggered PI control for continuous plants with input saturation," in *Proc. of American Control Conf.*, 2016, pp. 4251–4256.

[14] J. G. Da Silva, W. F. Lages, and D. Sbarbaro, "Event-triggered PI control design." in *Proc. of the 19th IFAC World Congress*, 2014, pp. 6947–6952.

[15] T. Norgren, J. Styrud, A. J. Isaksson, J. Åkerberg, and T. Lindh, "Industrial evaluation of process control using non-periodic sampling," in *Proc. of the 17th IEEE Conf. on Emerging Technologies and Factory Automation*, 2012, pp. 1–8.

[16] G. A. Kiener, D. Lehmann, and K. H. Johansson, "Actuator saturation and anti-windup compensation in event-triggered control," *Discrete Event Dynamic Systems*, vol. 24, no. 2, pp. 173–197, 2014.

[17] D. Lehmann, G. A. Kiener, and K. H. Johansson, "Event-triggered PI control: Saturating actuators and anti-windup compensation," in *Proc. of the 51st IEEE Conf. on Decision and Control*, 2012, pp. 6566–6571.

[18] D. Lehmann and K. H. Johansson, "Event-triggered PI control subject to actuator saturation," in *Proc. of the 2nd IFAC Conf. on Advances in PID Control*, 2012.

[19] S. Tarbouriech, G. Garcia, J. M. G. da Silva Jr, and I. Queinnec, *Stability and Stabilization of Linear Systems with Saturating Actuators*. Springer, 2011.

[20] N. P. Mahalik, *Sensor Networks and Configuration*. Springer, 2007.

[21] J. Löfberg, "Yalmip: A toolbox for modeling and optimization in matlab," in *Proc. of the 13th IEEE Int. Symp. on Computer Aided Control Systems Design*, 2004, pp. 284–289.